

The dependences of electroluminescent characteristics of ZnS:Mn thin films upon their device parameters

Hiroshi Sasakura, Hiroshi Kobayashi, Shosaku Tanaka, Juro Mita,^{a)}
Toshihiko Tanaka,^{b)} and Hirofumi Nakayama^{c)}
Department of Electronics, Tottori University, Koyama, Tottori 680, Japan

(Received 16 April 1981; accepted for publication 7 July 1981)

The dependences of brightness, emission efficiency η , average electric field E_A , conduction current J_A , and emission lifetime τ upon the device parameters such as film thickness, substrate temperature during evaporation, and Mn concentration have been systematically investigated in ZnS:Mn thin-film electroluminescent devices. The value of η increases rapidly with film thicknesses below 3000 Å but E_A decreases slowly. These results can be explained by the increase of the crystallinity of the ZnS:Mn films. The value of η increases with the Mn concentration and reaches its maximum at about 0.45 wt %. At above this Mn concentration, η and τ decrease rapidly, E_A increases, and J_A decreases slowly. These results may be attributed to a decrease of hot electron energy and/or an increase of the nonradiative transition probability of the excited Mn centers. The brightness-voltage (B - V) hysteresis characteristic is observed in this Mn concentration region. This memory effect is also discussed.

PACS numbers: 78.60.Fi 85.60.Jb

I. INTRODUCTION

Electroluminescent (EL) devices are available for completely solid displays. A large-area display can also be easily realized by use of these devices. Because of their high brightness and long life,^{1,2} many studies have recently been made of thin-film EL devices consisting of a ZnS:Mn layer sandwiched between two insulating layers.¹⁻¹¹ However, our information about the mechanism of electroluminescence in devices of this type is not yet sufficient, even though several studies on this mechanism have been already carried out.^{4,5,8,12} In order to elucidate the mechanism of electroluminescence, it is necessary to make careful studies on the dependences of various EL characteristics on various device parameters. Among the various EL characteristics of the devices, brightness and EL emission efficiency are the most important, but conduction current, electric field of the ZnS:Mn active layer, and decay time of EL emission are also important. Several studies have been reported on the dependences of individual EL characteristics on the device parameters,^{4,8,10} for example, the dependence of brightness on Mn concentration.^{8,10} However, no systematic study has been carried out on the dependences of the above mentioned EL characteristics upon various device parameters.

We have systematically investigated the dependences of these EL characteristics of the devices upon the device parameters, such as film thickness of the ZnS:Mn active layer, substrate temperature during evaporation, and Mn concentration of the active layer. These quantities have a remarkable effect on the EL characteristics, especially the brightness and the EL emission efficiency. From the experimental

results obtained, the mechanism of electroluminescence of thin film EL devices having a sandwich structure is discussed, and then the relationships between the EL characteristics and the device parameters are considered. In addition, the dependences of memory characteristics on the device parameters have been measured, and the memory mechanism is also discussed.

II. EXPERIMENTAL METHOD

The EL device structure used in the present study is shown in Fig. 1. The devices were prepared by sequential depositions of Y_2O_3 , ZnS:Mn, Y_2O_3 again, and finally Al onto an indium-tin-oxide (ITO) coated glass plate. The ZnS:Mn film was used as an EL emission layer, and the Y_2O_3 films were used as insulating layers. All these depositions were carried out by electron beam evaporation. A mixture of ZnS powder and Mn metal was used as the evaporation source of the ZnS:Mn film. The Mn concentration strongly affects the brightness and the memory characteristics of the device prepared. In our experiments, the Mn concentration was varied from 0.03 to 10 wt%. However, the constant Mn concentration of 0.45 wt% was chosen unless otherwise mentioned, because this concentration exhibits the maxi-

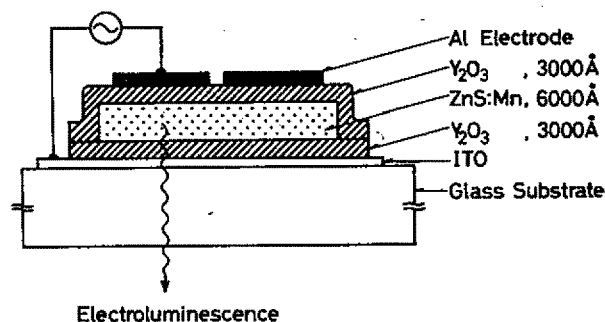


FIG. 1. Typical structure of a ZnS:Mn EL device.

^{a)}Present address: Oki Electric Industries, Co., Ltd., Toranomon, Minato-ku, Tokyo 105, Japan.

^{b)}Present address: Tottori Sanyo Electric Co., Ltd., Tachikawa, Tottori 680, Japan.

^{c)}Present address: Sony Co., Kitashinagawa, Shinagawa-ku, Tokyo 141, Japan.

imum efficiency as well as the strongest brightness. The thickness of the ZnS:Mn film and the substrate temperature during evaporation were varied from 700 to 8000 Å and 50 to 160 °C, respectively. The substrate temperature during evaporation of Y₂O₃ was 50 °C. The thickness of each Y₂O₃ insulating film was 3000 Å, which is the minimum value necessary to obtain stable operation of the device.

The EL characteristics were measured under the condition of driving the devices with 1 KHz sinusoidal excitation unless otherwise mentioned. When the ac applied voltage is lower than the threshold voltage for EL emission, a large displacement current, and a small conduction current which is due to the losses of the electrodes and the insulating layers, flow in the ac EL device. When the applied voltage exceeds the threshold voltage, the conduction current, sometimes called the dissipative current, begins to increase rapidly. In the present study, the instantaneous change and the time average of the conduction current were measured by a bridge circuit composed of the EL device and a capacitor having a capacitance equal to that of the EL device. The relative EL emission efficiency η was calculated as the ratio of the relative emission intensity to the real power loss in the EL device.

III. RESULTS AND DISCUSSION

A. Crystallinity of ZnS:Mn EL emission layers

In general, the crystallinity and orientation of evaporated films strongly depend on evaporation conditions such as substrate temperatures and underlying materials. In order to study the crystallinity of the ZnS:Mn EL layers, glass-ITO-Y₂O₃-ZnS:Mn multilayer films were prepared as samples for x-ray diffraction measurements in our work. The x-ray diffraction patterns of these samples are shown in Fig. 2. Substrate temperatures during evaporations of the ZnS:Mn films were 120 and 50 °C, and the thicknesses of both these films were 6000 Å. As shown in Fig. 2(a), the ZnS:Mn thin film evaporated at a substrate temperature of 120 °C shows

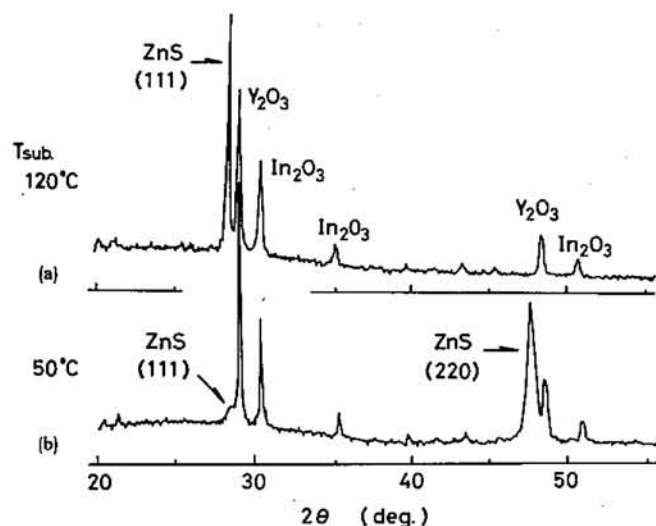


FIG. 2. X-ray diffraction patterns of the ZnS:Mn films using a Cu K α line. Substrate temperatures during evaporation are 120 and 50 °C, as shown in (a) and (b), respectively.

TABLE I. The x-ray diffraction intensities I_{111}^* and I_{220}^* of the ZnS:Mn films and the EL maximum efficiency η_{\max} (see Fig. 4) of the devices. The data have been obtained at several substrate temperatures during evaporation. The I_{111}^* and I_{220}^* are the intensities of the (111) and (220) lines per unit film thickness, respectively.

T_{sub} (°C)	I_{111}^*	I_{220}^*	η_{\max}
50	0.4	9.3	0.28
120	3.4	...	14.6
160	9.0	...	18.3

only the (111) line of the cubic structure of ZnS. In other words, the ZnS:Mn film strongly orientates its {111} surface parallel to the substrate. All other lines observed in the diffraction pattern are due to underlying Y₂O₃ and In₂O₃ films. Similar results have also been obtained for the ZnS:Mn films evaporated at substrate temperatures from 80 to 160 °C. In our experiment, it was difficult to grow ZnS film at substrate temperatures above 200 °C. As shown in Fig. 2(b), we found that the strong (220) line and the weak (111) line are observed for the ZnS:Mn film evaporated at a substrate temperature of 50 °C. These results show that the orientation of ZnS:Mn films strongly depends on the substrate temperature during evaporation. Recently the hexagonal structure of a ZnS film, which was prepared at a substrate temperature above 350 °C by the use of the atomic-layer epitaxy method, has been reported.¹³

Table I shows the x-ray diffraction intensities per unit thicknesses I_{111}^* , I_{220}^* , and the relative EL maximum efficiencies η_{\max} of the devices having these ZnS:Mn films. The value of η_{\max} was determined from the dependence on applied voltage, as described in Sec. III B. The ZnS:Mn films were prepared at the substrate temperatures T_{sub} 50, 120 and 160 °C. As shown in Table I, I_{111}^* rapidly increases with the substrate temperature. Simultaneously, η_{\max} also increases

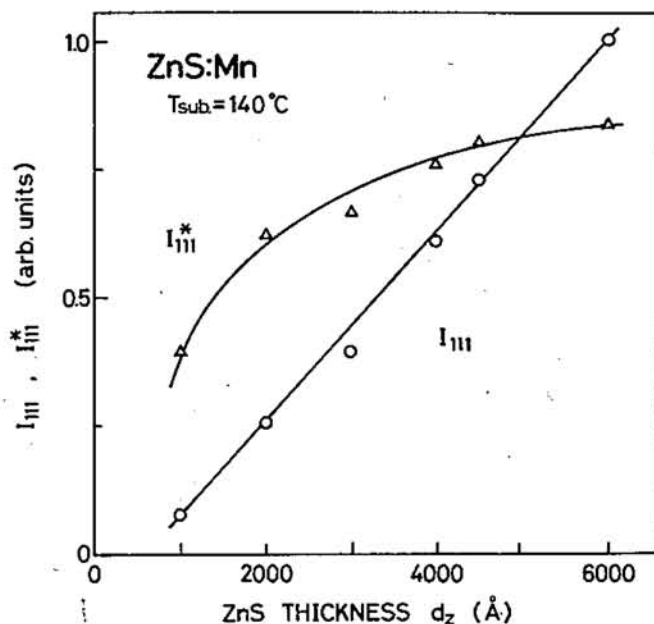


FIG. 3. Dependences of I_{111} and I_{111}^* on the thickness of the ZnS:Mn film, where I_{111} is the intensity of the (111) line and I_{111}^* is the intensity of the (111) line per unit thickness.

with the substrate temperature. This result strongly suggests that η_{\max} depends on the crystallinity of the ZnS:Mn films.

The dependence of the intensity of the (111) line I_{111} upon the film thickness of the ZnS:Mn d_z was measured in the case of the films prepared at the substrate temperature T_{sub} of 140 °C. Only the (111) line is observed in this preparation condition, and the (220) line is not observed. The result is shown in Fig. 3. The intensity per unit thickness I_{111}^* is also shown. The (111) line is hardly observed at film thicknesses below 1000 Å. The (111) line appears at about 1000 Å, and I_{111} increases linearly with increasing film thickness. Therefore, I_{111}^* rapidly increases in the neighborhood of a film thickness of 1000 Å, and tends to saturate gradually above about 4000 Å. The saturation of I_{111}^* with increasing film thickness is explained as follows. In the neighborhood of the ZnS/Y₂O₃ interface, the crystallinity of the ZnS:Mn film is not good, because the lattice constant of ZnS ($a = 5.4060$ Å) is about 2% larger than that of Y₂O₃ ($a/2 = 5.30$ Å). When the ZnS:Mn film grows larger than 1000 Å, the crystallinity of the film becomes better, and the {111} plane of ZnS begins to orientate parallel to the substrate. Therefore, I_{111}^* increases with the film thickness, and it eventually saturates at film thicknesses above 4000 Å.

B. The dependences of the brightness and the EL emission efficiency on the ZnS:Mn film thickness

The dependences of the brightness B and the relative EL emission efficiency η on the applied voltage are shown in Fig. 4, where the thickness of the ZnS:Mn film d_z is chosen as a parameter. The Mn concentration was 0.45 wt% and the substrate temperature during evaporation was 140 °C. When the film thickness is 6900 Å, the brightness B increases rapidly at an applied voltage of 140~170 V, and it tends to saturate above 200 V. The maximum brightness of about 1000 fL is obtained at an applied voltage of 230 V. However, the maximum efficiency η_{\max} is obtained at about 170 V. When the film thickness is 1400 Å, η_{\max} is obtained at about 130 V. When the film thickness is decreased to 700 Å, η_{\max} is obtained at about 150 V, which is slightly higher than that of the film thickness 1400 Å. In discussing the dependence of the brightness on the film thickness, we define the brightness B_A at the voltage V_A , at which η_{\max} is obtained (see Fig. 4). The electric field of the ZnS:Mn layer is nearly clamped above V_A .^{3,14,15} To discuss the film thickness and the Mn concentration dependences of the electric field, therefore, we use the electric field E_A at V_A , which is considered to be a representative value of the electric field. Strictly speaking, the ZnS:Mn film is not homogeneous as described below so that the electric field within it is not constant. However, for simplification, we may define E_A as the average electric field in the film. We have measured the electric field E_A by measuring the instantaneous conduction current,¹⁴ and also estimated E_A from the average conduction current. The value of E_A obtained with the above two methods coincided well with each other. The voltage V_A decreases when the thickness of the ZnS:Mn film is changed from 700 to 1400 Å. This result clearly shows that the electric field of the film decreases with the film thickness at least in the above-men-

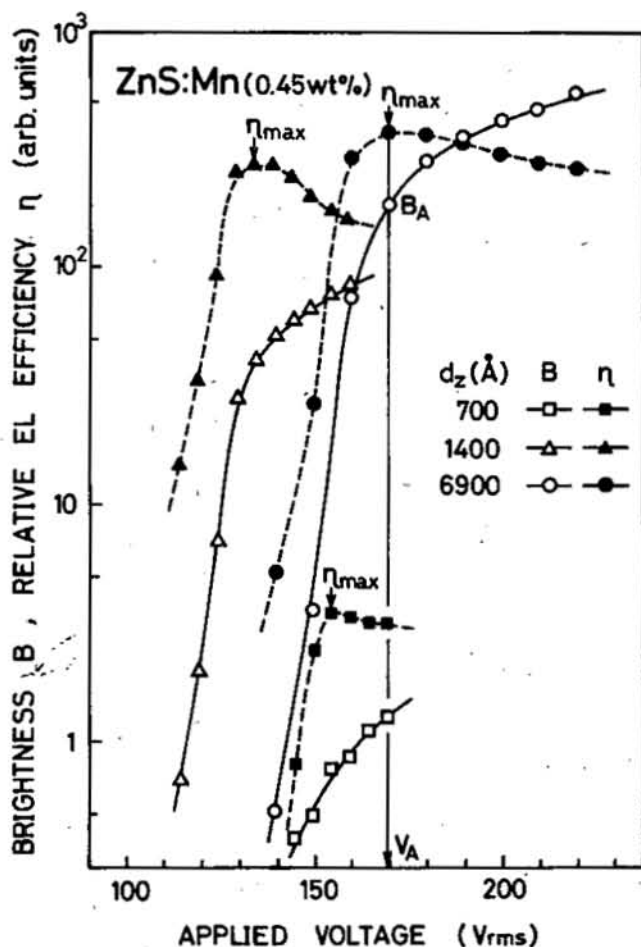


FIG. 4. Voltage dependences of brightness B and relative EL emission efficiency η . The thickness of the ZnS:Mn film d_z is taken as a parameter. The B_A and V_A obtained at η_{\max} are also shown in the case of d_z 6900 Å.

tioned range of film thicknesses, although the brightness and the EL emission efficiency increase.

Figure 5 shows the dependences of B_A , η_{\max} , and E_A on the thickness of the ZnS:Mn film d_z , together with I_{111}^* , which has already been shown in Fig. 3. The value of E_A is about 3×10^6 V/cm at a film thickness d_z of 700 Å. As described above, E_A decreases gradually with increasing d_z and reaches about 1.5×10^6 V/cm at d_z 3000 Å. In any further increase of d_z , E_A remains nearly constant. On the other hand, B_A first increases rapidly with an increasing d_z , and it increases nearly proportionally to d_z above 3000 Å. The maximum EL efficiency η_{\max} increases rapidly from a film-thickness d_z of 700 Å and reaches its largest value at a d_z of about 3000 Å. The increase of the η_{\max} is more than 10^2 times in this film thickness range. In any further increase of d_z , η_{\max} keeps nearly constant. I_{111}^* increases gradually with increasing d_z , and it stays at nearly a constant value above 3000 Å. The tendency of variation of I_{111}^* with increases in d_z is similar to that of η_{\max} . The increase of I_{111}^* gives direct evidence that the crystallinity of the ZnS:Mn film improves with increased film thickness. Therefore, it seems very likely that a close correlation exists between η_{\max} and the crystallinity of the ZnS:Mn film. It has been already reported that the low EL emission efficiency of ZnS:Mn film is observed at film thicknesses below 2000 Å, and it has been suggested that

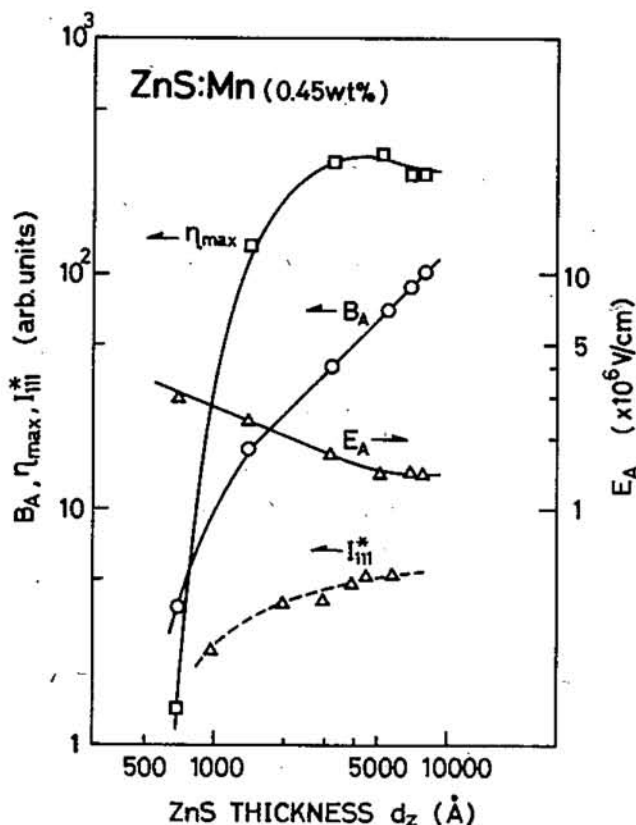


FIG. 5. Dependences of brightness B_A , the maximum EL emission efficiency η_{\max} , and the electric field of the ZnS:Mn film E_A upon the film thickness of the ZnS:Mn active layer. The B_A and E_A are measured at the voltage V_A , at which η_{\max} is obtained. The dependence of I_{11}^* is also shown.

this low EL efficiency may be correlated to the crystal morphology of the ZnS:Mn film.^{12,16} Our results are well consistent with this suggestion.

The close correlation between η_{\max} and the crystallinity of the ZnS:Mn film can be explained as follows. As the excitation mechanism is due to impact excitation by hot electrons,⁵ η_{\max} depends on the energy distribution of the hot electrons. This distribution can be represented as a function of $eE_A\lambda$,^{14,17} where e is a charge of an electron and λ is the mean free path of hot electrons. From the analysis, it is clear that η_{\max} increases rapidly when $eE_A\lambda$ increases slightly.

We first discuss the dependence of E_A and λ on the crystallinity, which in turn depends on the film thickness. In general, λ is considered in homogeneous material. However, the ZnS:Mn EL emission layer is an inhomogeneous layer, in which the crystallinity becomes better the greater the distance from the ZnS/Y₂O₃ interface. It is well-known that λ increases when the crystallinity of a solid improves. Therefore, λ can be regarded as increasing with increasing distance from the ZnS/Y₂O₃ interface in the ZnS:Mn layer. As the average energy of hot electrons increases with increasing λ , it increases with increasing film thickness, so that the avalanche breakdown field E_A (Ref. 15) is expected to become lower. This expectation agrees with the present experimental results concerning E_A .

We next discuss the maximum efficiency η_{\max} . As described above, η_{\max} is also the function of $eE_A\lambda$ and increases rapidly when $eE_A\lambda$ increases even slightly.¹⁴ With an

increasing film thickness, λ increases and E_A decreases. The observed decrease of E_A is from 3×10^6 to 1.5×10^6 V/cm by increasing the film thickness from 700 to 3000 Å. In other words, E_A is reduced to about half its former value in this range of film thicknesses. However, if λ becomes 3~5 times larger at that time, $eE_A\lambda$ becomes about twice as large. From this, one can explain the observed increase of η_{\max} of about 10^2 times as being due to the increase of $eE_A\lambda$.

C. Dependences of B_A , η_{\max} , E_A , J_A , and τ on the Mn concentration

Figure 6 shows the dependences of B_A , η_{\max} , and E_A on the Mn concentration of the ZnS:Mn EL active layer. The Mn concentration was varied from 0.03 to 10 wt%. The ZnS:Mn film of thickness 6000 Å was prepared at the substrate temperature 140 °C during evaporation. The applied voltage dependence of the average conduction current J has been measured, and it increases nearly proportionally to $(V - V_{th})$, where V_{th} is the threshold voltage for EL emission. Figure 6 also shows the concentration dependences of the conduction current J_A , defined at the voltage V_A , because it is a current under the electric field E_A at which the avalanche breakdown begins to occur in the ZnS:Mn layer. This value seems to be useful in discussing conduction mechanisms of ZnS:Mn EL layers having various Mn con-

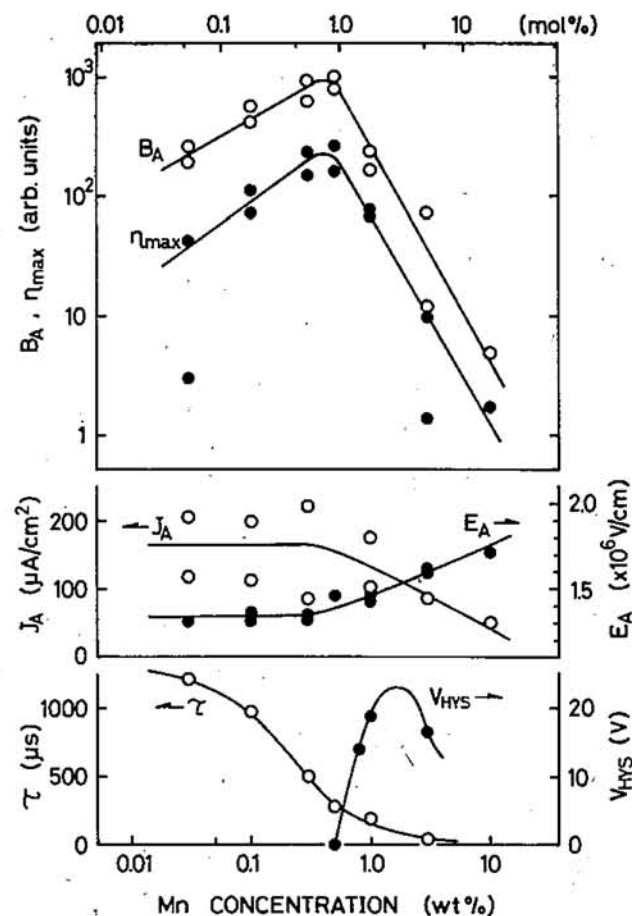


FIG. 6. Dependences of B_A , η_{\max} , E_A , J_A , and τ on the Mn concentration of the ZnS:Mn active layer, where J_A is the conduction current density of the active layer and τ is the decay time of EL emission. The dependence of the hysteresis width V_{HYS} on the Mn concentration is also shown.

centrations. The decay time of the Mn electroluminescence τ , which is measured by applying the pulse voltage (rise time $< 10 \mu\text{s}$, pulse width $\sim 100 \mu\text{s}$) to the device, is also shown in Fig. 6.

In the region of low Mn concentration, B_A and η_{max} increase with increasing Mn concentration and reach maximum at an Mn concentration of 0.45 wt%. Unlike B_A and η_{max} , J_A and E_A are nearly constant when the Mn concentration is below 0.5 wt%, but J_A begins to decrease and E_A begins to increase as the Mn concentration becomes higher. Furthermore, the larger conduction current J at a higher voltage than V_A tends to decrease with Mn concentration as well as J_A . The brightness-voltage ($B-V$) hysteresis characteristic, the so-called memory effect,² is observed when the device has an Mn concentration of more than 0.5 wt%. The hysteresis voltage width V_{HYS} is also shown in Fig. 6. This memory effect is discussed in Sec. III D.

In this section, the dependences of E_A and J_A on the Mn concentration are first discussed. E_A is considered to be determined by the avalanche breakdown process.¹⁵ In our experiment, E_A increased with increasing Mn concentration. Similar behavior of a threshold electric field has also been observed recently.⁸ From our observation, it seems that the mean free path of electrons λ may decrease in the high Mn concentration region, because the avalanche breakdown of the ZnS:Mn layer having higher Mn concentration occurs in higher electric fields, as long as the value of $eE_A\lambda$ keeps to a certain value. The decrease of λ is presumably due to the increase of the scattering probability of hot electrons by Mn centers and/or the decrease of the crystallinity in the ZnS:Mn layer. On the other hand, J_A decreases with increasing Mn concentrations. We may point out that there are two possible causes for the decrease of J_A . One is a decrease of the electron density and the other is a decrease in the length of the mean free path. However, our knowledge of the conduction mechanism in ZnS:Mn under high electric fields is still insufficient to enable us to draw a valid conclusion.

Next, the dependences of B_A and η_{max} on the Mn concentration are discussed. In the low Mn concentration region below 0.3 wt%, both B_A and η_{max} increase with the Mn concentration. In this concentration region, E_A and J_A are nearly constant, that is to say, the energy distribution of hot electrons in the ZnS:Mn layer does not change much. Therefore, one may attribute the increase of B_A and η_{max} to the increase of Mn luminescence centers. In the high Mn concentration region above 0.5 wt%, both B_A and η_{max} decrease rapidly. Two mechanisms may be responsible for the decrease of η_{max} . One is the decrease of the mean free path of electrons, which is due to the scattering of hot electrons by the Mn centers and/or the decrease of the crystallinity in the ZnS:Mn layer. The other is the increase of the nonradiative transition probability of the excited Mn centers. The existence of a nonradiative transition process is plausible, because the decrease in the decay time τ of the Mn EL emission was observed in our experiments. Both mechanisms are present in the electroluminescence of the ZnS:Mn film, but it is not yet clear which mechanism is predominant.

Further, we have investigated the dependences of B_A , η_{max} , E_A , J_A , and τ on the Tb concentration in ZnS:TbF₃

films. Preliminary results show that the dependences of these quantities (except for τ) on the Tb concentration are similar to the case of ZnS:Mn films. In ZnS:TbF₃ films, τ increases with the Tb concentration, which is contrary its behavior in ZnS:Mn films. A detailed analysis and comparison of the dependences of B_A , η_{max} , J_A , E_A , and τ upon the Mn and Tb concentrations will give us a clearer knowledge of the mechanism of electroluminescence in ZnS films.

D. $B-V$ hysteresis characteristic

ZnS:Mn EL devices having a sandwich structure show the $B-V$ hysteresis characteristic when the Mn concentration is above 0.5 wt%. EL devices with a ZnS:Mn film thickness of 6000 Å and an Mn concentration of 0.7 wt% were prepared at the substrate temperature 140 °C during evaporation. The typical $B-V$ characteristic of the device is shown in the inserted figure in Fig. 7. The hysteresis width V_{HYS} is defined as the voltage width at about 1-fL brightness level on the hysteresis loop, as shown in the figure. The dependence of the hysteresis width on the Mn concentration has already been shown in Fig. 6 and its dependence on the film thickness is shown in Fig. 7. As already reported,^{4,8,10} V_{HYS} increases rapidly just above the threshold Mn concentration of 0.5 wt% and increases nearly proportionally to the increase of film thicknesses above 2000 Å.

Many studies have been reported and several mechanisms have been proposed about the memory effect.^{3,4,6-8,10,16} However, none of them seems to have been successful in giving a consistent and satisfactory explanation about the experimental results of the memory effect, such as the dependences of the hysteresis width on the Mn concentration and the film thickness. Here, we wish to discuss the mechanism of the memory effect, taking into account our experimental results with ZnS:TbF₃ EL devices, since ZnS:TbF₃ devices show no memory effect even if the Tb

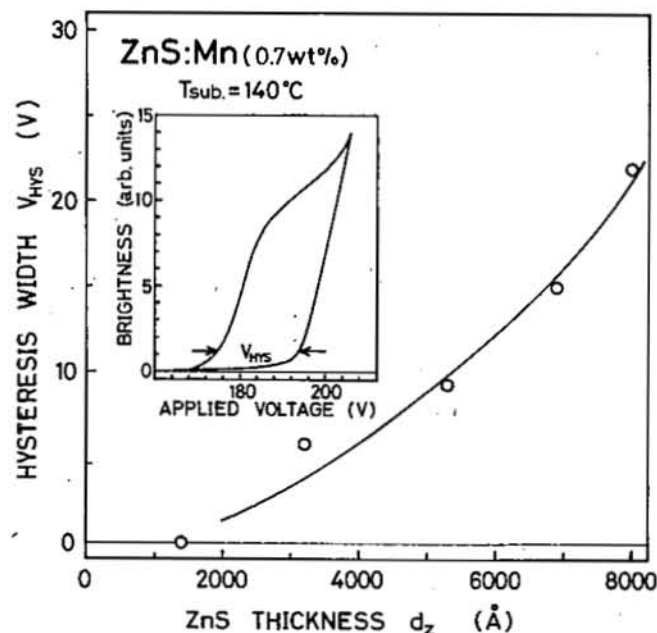


FIG. 7. Dependence of hysteresis width V_{HYS} on the film thickness of the ZnS:Mn active layer of the device. The typical $B-V$ hysteresis characteristic of the device is also shown in the inserted figure.

concentration exceeds 5 wt%. In the higher concentration region, both ZnS:Mn and ZnS:TbF₃ devices show an increase of E_A and a decrease of J_A . However, the hysteresis of the conduction charge is observed only in the ZnS:Mn devices. The decrease of τ is also observed in the ZnS:Mn devices, that is, the nonradiative transition probability increases in the concentration region of the memory effect. This indicates that Mn complexes¹⁸ are formed (as killer centers) in the higher Mn concentration-region. Therefore, the main cause of the hysteresis characteristics observed in the ZnS:Mn devices is presumably the electron traps of the Mn complexes, which are formed in the ZnS:Mn layer at higher Mn concentrations. However, the memory effect is a very complicated phenomenon, and further detailed study is necessary for a more perfect understanding of its nature.

IV. SUMMARY

We have investigated systematically the dependences of the electroluminescent characteristics of ZnS:Mn EL thin-film devices upon the device parameters, such as crystallinity, film thickness, and Mn concentration of the ZnS:Mn active layer. The results are summarized as follows.

(1) The {111} surface of the cubic-ZnS:Mn film is parallel to the substrate at substrate temperatures during evaporation of 80~160 °C. The substrate temperature affects the crystallinity of the films. The x-ray diffraction intensity I_{111}^* increases with the film thickness, and it tends to saturate above 3000 Å. The increase of I_{111}^* shows that the crystallinity increases with the film thickness.

(2) In the region of film thicknesses below 3000 Å, the maximum EL emission efficiency η_{max} increases. However, the average electric field of the ZnS:Mn layer decreases with the film thickness. The increase of η_{max} can be explained by the increase of the mean free path λ , when the crystallinity increases with the film thickness.

(3) With increasing Mn concentration, η_{max} increases and reaches maximum at about 0.45 wt%. With any further increase of the Mn concentration, η_{max} and τ decrease rapidly. Also, E_A increases slowly and J_A decreases slowly. These results may be attributed to the decrease of hot electron ener-

gy in the ZnS:Mn active layer and the increase of the nonradiative transition probability of the excited Mn emission centers.

(4) The B - V hysteresis characteristic, the so-called memory effect, is observed in devices with Mn concentrations above 0.5 wt% and film thicknesses above 2000 Å. The mechanism of this effect is probably related to the variation of E_A and J_A , and to the formation of Mn-complex centers. However, the mechanism is too complicated for a completely satisfactory understanding.

¹T. Inoguchi, M. Takeda, Y. Kakihara, Y. Nakata, and M. Yoshida, Digest 1974 SID International Symposium (Society for Information Display, Los Angeles, 1975), p. 84.

²Y. Yamauchi, M. Takeda, Y. Kakihara, M. Yoshida, J. Kawaguchi, H. Kishishita, Y. Nakata, T. Inoguchi, and S. Mito, Digest 1974 Int. Elec. Device Mtg. (IEEE, New York, 1974), p. 352.

³M. Takeda, Y. Kakihara, M. Yoshida, Y. Nakata, M. Kawaguchi, H. Kishishita, Y. Yamauchi, T. Inoguchi, and S. Mito, J. Jpn. Soc. Appl. Phys. **44** (Suppl.), 103 (1975).

⁴M. Yoshida, Y. Kakihara, T. Yamashita, K. Taniguchi, and T. Inoguchi, Jpn. J. Appl. Phys. **17** (Suppl. 17-1), 127 (1978).

⁵S. Tanaka, H. Kobayashi, H. Sasakura, and Y. Hamakawa, J. Appl. Phys. **47**, 5391 (1976).

⁶V. Marrello, W. Rühle, and A. Onton, Appl. Phys. Lett. **31**, 452 (1977).

⁷W. Rühle, V. Marrello, and A. Onton, J. Lumin. **18/19**, 729 (1979).

⁸V. Marrello and A. Onton, IEEE Trans. Electron Devices **ED-27**, 1767 (1980).

⁹W. E. Howard, IEEE Trans. Electron Devices **ED-24**, 903 (1977).

¹⁰J. M. Hurd and C. N. King, J. Electron. Mater. **8**, 879 (1979).

¹¹J. Benoit, P. Benaiouil, R. Parrot, and J. Mattler, J. Lumin. **18/19**, 739 (1979).

¹²V. Marrello and A. Onton, Appl. Phys. Lett. **34**, 525 (1979).

¹³V.P. Tanninen, T. Tuomi, M. C. Typpi, R. O. Törnqvist, T. Suntola, J. Antson, A. Pokkala, and S. Lindfors, in (Proceedings of the 8th International Vacuum Congress, Cannes, 1980), p. 401.

¹⁴Y. S. Chen and D. C. Krupka, J. Appl. Phys. **43**, 4089 (1972).

¹⁵H. Kobayashi, S. Tanaka, H. Sasakura, and Y. Hamakawa, Jpn. J. Appl. Phys. **13**, 264 (1974).

¹⁶V. Marrello and A. Onton, J. Electrochem. Soc. **127**, 2220 (1980).

¹⁷G. A. Baraff, Phys. Rev. A **133**, 26 (1964).

¹⁸W. Busse, H. E. Gumlich, B. Meissner, and D. Thesis, J. Lumin. **12/13**, 693 (1976).